Efficiency of Gas-Phase Ion Formation in Matrix-Assisted Laser Desorption Ionization with 2,5-Dihydroxybenzoic Acid as Matrix

Kyung Man Park, Sung Hee Ahn, Yong Jin Bae, and Myung Soo Kim*

*Department of Chemistry, Seoul National University, Seoul 151-742, Korea. *E-mail: myungsoo@snu.ac.kr*
Received December 1, 2012, Accepted December 26, 2012

Numbers of matrix- and analyte-derived ions and their sum in matrix-assisted laser desorption ionization (MALDI) of a peptide were measured using 2,5-dihydroxybenzoic acid (DHB) as matrix. As for MALDI with α-cyano-4-hydroxy cinnamic acid as matrix, the sum was independent of the peptide concentration in the solid sample, or was the same as that of pure DHB. This suggested that the matrix ion was the primary ion and that the peptide ion was generated by matrix-to-peptide proton transfer. Experimental ionization efficiencies of 10^{-5}-10^{-4} for peptides and 10^{-8}-10^{-7} for matrices are far smaller than 10^{-3}-10^{-1} for peptides and 10^{-5}-10^{-3} for matrices speculated by Hillenkamp and Karas. Number of gas-phase ions generated by MALDI was unaffected by laser wavelength or pulse energy. This suggests that the main role of photo-absorption in MALDI is not in generating ions *via* a multi-photon process but in ablating materials in a solid sample to the gas phase.

Key Words : MALDI, 2,5-Dihydroxybenzoic acid, Ionization efficiency, Ion formation mechanism, Laser fluence and wavelength dependences

Introduction

Matrix-assisted laser desorption ionization (MALDI)[1-3] is widely used in mass spectrometry for biological molecules. However, how gas-phase ions are formed in MALDI is not well established. Among the hypotheses proposed so far, the two step mechanism seems to be generally accepted for MALDI of many biological molecules such as peptides that will be dealt with in this work.[4] In this mechanism, gas-phase matrix ions ($[M + H]^+$) are produced *via* a primary process(es). Then, the matrix-to-analyte proton transfer generates the analyte ion ($[A + H]^+$).

The hypotheses proposed to explain the primary process can be divided into two groups depending on the role of photo-excitation in MALDI. In the first group of hypotheses, photo-excitation of neutral matrix molecules eventually induces their ionization from a highly excited electronic state.[4,5] In contrast, in the second group, photo-excitation is simply an instantaneous way of supplying thermal energy to the sample and hence inducing its ablation.[6-9] The thermal energy needed for ablation is supplied by photo-excitation in the first group of hypotheses also. Ionization of matrix molecules *via* pooling of excitons is the leading hypothesis belonging to the first group, while thermal processes such as the pre-formed ion emission have been proposed for the second group.[4]

Recently, we measured the number of gas-phase ions generated in MALDI of peptides using α-cyano-4-hydroxy-cinnamic acid (CHCA) as matrix.[9] Two important observations were made in the study. One was that the total number of gas-phase ions appearing in a MALDI spectrum, *viz.* the sum of the abundances of matrix (M)- and peptide (P)-derived ions, was independent of the peptide concentration in the solid sample, and hence was the same as that from

pure CHCA. That is, the increase in the total abundance of analyte-derived ions is matched by the decrease in that of matrix-derived ions. This is consistent with the hypothesis in the two step model that the proton transfer from $[M + H]^+$ to P in the second step produces $[P + H]^+$. The other observation was that the total number of gas-phase ions was independent of the laser pulse energy - with the laser focusing optics fixed, pulse energy is almost proportional to fluence. Apparently, this is inconsistent with the first group of hypotheses that postulate laser-induced ionization of matrix molecules as the mechanism for the primary ion formation.

2,5-Dihydroxybenzoic acid (DHB) is a molecule that is also widely used as matrix. In fact, CHCA and DHB are the two most popular matrices in MALDI.[1,3] One of the important differences between the two is in their influence on the dissociation of analyte ions, CHCA inducing more extensive dissociation than DHB does both inside (in-source decay, ISD) and outside (post-source decay, PSD) the ion source.[10] Another is that DHB is far more effective in generating c and z type product ions in ISD of peptides.[11,12]

As far as the mechanism for the gas-phase ion formation in MALDI is concerned, the main interest in DHB lies in the fact that this is the only system for which the exciton pooling model has been tested through molecular dynamics simulation.[13] In this regard, it is of interest to check whether the fluence independence of the ionization efficiency observed for CHCA-MALDI will also hold for DHB-MALDI. Unlike CHCA, however, it is difficult to prepare a rather homogeneous sample of DHB, a problem in the determination of the ionization efficiency.[14] Recently, we found that we could overcome this by using pre-spotted DHB-MALDI plates.[15] The results from the measurements and their implication on the mechanism for gas-phase ion formation in MALDI will be presented in this paper.

Experimental

Details of the homebuilt MALDI mass spectrometer were reported previously.[10,16] The instrument consists of an ion source with delayed extraction, a linear time-of-flight (TOF) analyzer, an ion gate, a second-stage analyzer equipped with a reflectron with linear-plus-quadratic (LPQ) potential inside, and a microchannel plate detector (MCP, #31849, Photonis USA, Sturbridge, MA, USA). In addition to the prompt ions and their ISD products, PSD products of the prompt ions and those of ISD products appear in an ordinary MALDI-TOF spectrum recorded by the apparatus.[10] Hence, the total abundances of the matrix and analyte ions generated by MALDI can be measured from a single mass spectrum. The method to calculate the number of ions in each peak, including the method for detector gain calibration, was reported previously.[17] With eleven grids on the ion path, the theoretical transmission of the instrument is 0.286.

Output of a dye laser (ND 6000, Continuum, Santa Clara, CA) pumped by a Nd:YAG laser (PL8010, Continuum, Santa Clara, CA) was frequency-doubled to generate MALDI laser at 317 (DCM dye), 337 (DCM + pyridine 1), and 357 nm (pyridine 1 + pyridine 2). Shape of the laser beam was manipulated such that the major and minor diameters of the ellipse at the sample spot became 180 and 85 μm, respectively, regardless of the wavelength. The threshold laser pulse energy for MALDI was determined following the method reported previously.[18] They were 2.3 ± 0.2, 1.7 ± 0.2, and 1.6 ± 0.1 μJ/pulse at 317, 337, and 357 nm, respectively (Table 1).

Samples. Peptide YYYYYR (Y_5R) was purchased from Peptron (Daejeon, Korea). Pre-spotted DHB plates for MALDI were purchased from Asta (Suwon, Korea). The area of each DHB sample printed on each plate was 2.6 mm^2. To determine the amount of DHB in each circular sample, it was extracted with water several times. DHB in the aqueous solution thus collected was quantified by UV absorption spectroscopy, resulting in 85 ± 3 nmol DHB in each sample. Y_5R was dissolved in aqueous solution of 80% acetonitrile. 1.0 μL of the solution was loaded on each pre-spotted DHB sample and vacuum-dried. The amount of Y_5R in a sample was 0-90 pmol.

Method

The method to determine the number of gas-phase ions generated from a solid sample by MALDI was described in details previously.[9,17] A brief account is as follows.

We noted that determining this number by measuring the total number of ions emitted from the whole area of a sample or by utilizing the result from a laser focal spot might be difficult and/or erroneous. Instead, we decided to measure the total number (N_P) of ions emitted from an area (A_P) larger than that of a laser focal spot and convert it to the total number (N_S) of gas-phase ions expected from the whole sample with the area A_S by $(A_S/A_P)N_P$. For this purpose, we completely depleted samples at a laser focal spot by repetitive irradiation with sufficiently large pulse energy and moved the focal spot, eventually drawing a burn mark of a parallelogram (280 μm × 200 μm) on a sample. Decent homogeneity of a sample is a requirement for the reliability of this method. To check the homogeneity of a sample obtained by loading Y_5R on pre-spotted DHB, we measured the total number of ions generated from some laser focal spots on a sample. The measurement at each spot was made until it was completely depleted by repetitive laser irradiation. The spot dependence of the total ion signal was tolerable as can be seen in Figure 1.

As mentioned earlier, the total charge for each ion signal in a spectrum was converted to the number of ions by utilizing the result from detector gain calibration.[19] We also
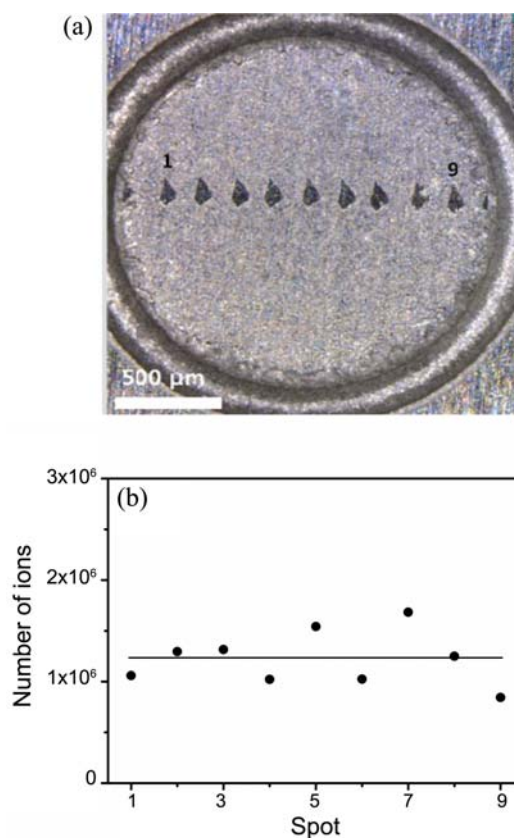

Figure 1. (a) Nine burn marks on a pre-spotted DHB sample are shown where the total numbers of emitted ions were measured. The sample contained 10 pmol of Y_5R in 85 nmol DHB. Six times the threshold laser pulse energy was used. (b) The number of ions, *i.e.* the sum of DHB- and Y_5R-derived ions, from each spot. The horizontal line denotes the average.

Table 1. Absorption coefficients^a of DHB in the 317-357 nm spectral range and threshold laser pulse energies for MALDI with DHB

Matrix		317 nm	337 nm	357 nm
DHB	Absorption coefficient (10^4 cm^{-1})	6.0	8.4	8.7
	Threshold laser energy (μJ/pulse)	2.30 ± 0.17	1.65 ± 0.14	1.63 ± 0.07

^{a}Ref. 22

corrected for the ion loss due to post-source dissociation occurring in field regions simply by taking into account the times an ion spent in the field and field-free regions after coming out of the source.[9,17] For the total PSD ion signal estimated by this method, we expect ± 20% error. The associated error on the total number of ions would be much less. In particular, we did not have to worry about this error in the present work because the abundances of PSD product ions in DHB-MALDI of Y_5R were very small. Finally, we took into account 28.6% transmission through the apparatus and 62% entrance to microchannels in MCP.

Results and Discussion

Spectra. MALDI spectrum for pre-spotted DHB obtained at 337 nm is shown in Figure 2(a). 9.9 μJ/pulse of laser energy, corresponding to six times the threshold, was used. Protonated DHB and related ions form prominent features in the spectrum, *viz.* $[DHB + H]^+$, $[DHB + H - H_2O]^+$, and $[2DHB + H - 2H_2O]^+$. The radical cation, $DHB^{+\bullet}$, also appears. In addition, alkali metal adducts such as $[DHB + Na]^+$, $[DHB + K]^+$, and $[DHB + Na - H_2O]^+$ appear. MALDI spectrum obtained by loading 10 pmol of Y_5R on the pre-spotted DHB is shown in Figure 2(b). Compared to CHCA-MALDI spectrum of the same peptide,[9] not as many ISD and PSD product ions appear in DHB-MALDI and the abundances of those appearing in the spectrum are smaller. This is due to the well-known fact that DHB is a colder matrix than CHCA.[1,10] Among the ISD products, immonium ion R is the most prominent, but contributes only 4% to the total abundance of peptide-derived ions. Other ISD products such as immonium Y and y_4 were much weaker. Among the PSD product ions, only $y_1 - NH_3$ made any significant contribution (3%) to the ion yield data. We would like to add that we searched for but failed to observe matrix-peptide cluster ions.

Number of Gas-Phase Ions *vs.* Sample Composition. The total numbers of DHB- and Y_5R-derived ions and their sum measured as a function of the peptide concentration in solid sample are listed in Table 2. The measurement was made using 337 nm output of a dye laser with 9.9 μJ/pulse corresponding to six times the threshold. We assumed that the matrix-to-peptide proton transfer, *i.e.* $[M + H]^+ + P \rightarrow M$

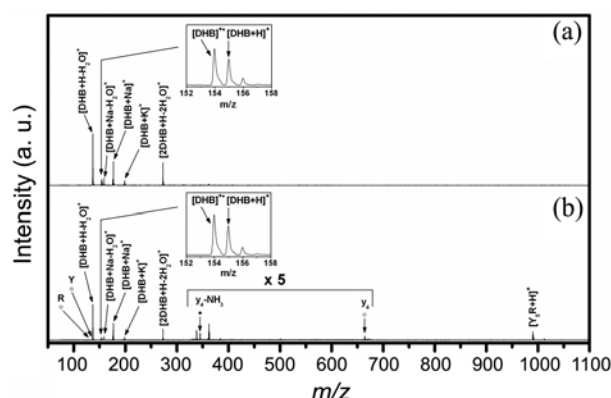**Figure 2.** MALDI spectra for (a) pure DHB and (b) 10 pmol Y_5R in 85 nmol DHB obtained at 337 nm with 9.9 μJ/pulse corresponding to six times the threshold. Some matrix- and analyte-derived ions are marked. Open and filled circles represent ISD and PSD products, respectively, of the analytes.

$+ [P + H]^+$, was responsible for the peptide ion formation in MALDI. Accordingly, we included the abundances of proton donors in the calculation of the number of gas-phase ions produced. Specifically, alkali metal adducts and the radical cation of DHB were excluded from each sum. The numbers including these ions are added in the parentheses. In both cases, the total number of the matrix-derived ions decreases steadily as the peptide concentration in solid sample increases. As can be seen from the same table, the total number of ions appearing in MALDI spectra, *i.e.*, the sum of the numbers of matrix- and analyte-derived ions, is the same regardless of the analyte concentration in solid sample. Hence, as in CHCA-MALDI,[9] $[M + H]^+$ is the primary ion and the matrix-to-peptide proton transfer generates $[P + H]^+$. This conclusion seems to be valid even though the analyte-to-peptide alkali metal ion transfer also occurs in the present case. The fact that $[M + H]^+$ is the primary ion means that it suffices to deal with pure DHB, rather than DHB-analyte mixtures, in our investigation on the process(es) involved in the primary ion formation.

By dividing the number of the analyte-derived ions with the number of the analyte neutral in each solid sample, we obtained the ionization efficiency for the analyte *vs.* its

Table 2. The Numbers of Y_5R and DHB-derived positive ions, their sum, and ionization efficiencies of Y_5R and DHB *vs.* the amount[a] of Y_5R in DHB-MALDI

Y_5R, pmol	Number of ions from sample[b]			Ionization efficiency	
	Y_5R, 10^8	DHB, 10^9	Sum, 10^9	Y_5R, 10^{-5}	DHB, 10^{-8}
0	-	1.2±0.6 (2.2±0.7)	1.2±0.6 (2.2±0.7)	-	2.4±1.2 (4.2±1.4)
1	0.64±0.14(0.69±0.25)	1.1±0.2 (2.1±0.4)	1.1±0.3 (2.1±0.4)	11±4 (11±4)	2.1±0.5 (4.0±0.8)
3	1.6±0.6 (1.8±0.6)	1.2±0.4 (1.9±0.5)	1.3±0.5 (2.0±0.6)	9.0±2.0 (9.8±2.9)	2.3±0.8 (3.6±1.1)
10	3.3±0.8 (3.7±0.8)	0.93±0.15 (1.6±0.3)	1.3±0.2 (1.9±0.2)	5.5±0.8 (6.2±1.2)	1.8±0.3 (3.1±0.5)
30	8.8±1.0 (10±1)	0.66±0.23 (0.88±0.30)	1.5±0.4 (1.9±0.4)	4.9±0.5 (5.8±0.6)	1.3±0.4 (1.7±0.6)
60	9.6±3.7 (11±4)	0.56±0.19 (0.79±0.21)	1.5±0.6 (1.9±0.6)	2.6±1.0 (3.0±1.1)	1.1±0.2 (1.6±0.4)
90	14±6 (15±6)	0.52±0.03 (0.78±0.14)	1.7±0.3 (2.2±0.6)	2.5±1.1 (2.8±1.2)	1.0±0.2 (1.5±0.3)

[a]In 85 nmol of DHB. [b]Numbers inside parentheses include alkali metal ion adducts.

concentration. Similar data were obtained for DHB also. The results are listed Table 2. The ionization efficiency for pure DHB was around one fifth of that for CHCA, $(2.4 \pm 1.2) \times 10^{-8}$ for DHB *vs.* $(1.2 \pm 0.1) \times 10^{-7}$ for CHCA.[9] When compared at comparable concentrations, the ionization efficiency for Y_5R in DHB-MALDI was smaller than that in CHCA-MALDI by a factor of 3-4, for example, $(5.5 \pm 0.8) \times 10^{-5}$ for 10 pmol Y_5R in 85 nmol DHB *vs.* $(2.1 \pm 0.2) \times 10^{-4}$ for 3.0 pmol Y_5R in 25 nmol CHCA. As noted in our previous study, the ionization efficiencies of 10^{-5}-10^{-4} for analytes are consistent with the measurements by Mowry and Johnston.[20] Those of 10^{-8}-10^{-7} for matrices are smaller than 10^{-7}-10^{-6} estimated from the data reported by Sundqvist *et al.*[21] We would like to emphasize that both of them are smaller by orders of magnitude than 10^{-3}-10^{-1} for analytes and 10^{-5}-10^{-3} for matrices speculated by Hillenkamp and Karas.[1] Inaccurate information on the efficiency of gas-phase ion generation might partly be responsible for the fact that how ions are formed in MALDI is still an open question even after more than twenty years of its inception.

Number of Gas-Phase Ions *vs.* Laser Pulse Energy and Wavelength. If the gas-phase primary ion, $[M + H]^+$, is generated by a some form of laser-induced ionization such as the multi-photon ionization mediated by exciton pooling, the efficiency for its formation will increase with the photon energy density of the irradiated spot. The energy density will certainly increase with the laser pulse energy. Another factor that affects the energy density is the absorption coefficient. The absorption coefficients of DHB at the laser wavelengths adopted in this work are listed in Table 1 together with the thresholds.[22] The total number of DHB-derived ions and the ionization efficiencies, without and with alkali metal adducts, measured at several wavelength-pulse energy combinations are listed in Table 3. Taking MALDI at 337 nm as an example, the number of gas-phase matrix-derived ions is clearly independent of the laser pulse energy. In fact, the number of gas-phase ions, and hence the ionization efficiency also, do not show any dependence either on the laser wavelength or

on the pulse energy at each wavelength.

Mechanism for the Primary Ion Formation in MALDI. The fact that the ionization efficiency for DHB is independent of the pulse energy and wavelength of laser discredits the laser-induced ionization as the model for primary ion formation in MALDI. Specifically, ionization in an excited electronic state(s) accessed by photo-absorption, such as the one envisioned in the exciton pooling model, cannot be the mechanism for the ion formation in MALDI.

Even though the involvement of excited-state chemistry in MALDI has been rejected, one cannot deny the fact that the energy supplied *via* photo-absorption is the driving force of MALDI. For example, it is well known that the ion yield per laser pulse, that is negligible below a certain threshold value, suddenly increases rapidly at and above the threshold. Such an exponential increase in ion yield was often taken as evidence for the participation of a multi-photon process for ionization.[23] However, also well-known is the fact that the amount of materials emitted to the gas-phase in laser-induced ablation also increases rapidly with the laser pulse energy.[24] That is, with the primary ion formation *via* a multi-photon process discredited, the well-known threshold behavior in MALDI seems to be a manifestation of laser-induced ablation.

Conclusion

In our previous study on MALDI of peptides using CHCA as matrix, we found that the total number of gas-phase ions generated by MALDI was independent of the analyte concentration in the solid sample and the laser pulse energy. The first independence was taken as evidence for the peptide ion formation *via* matrix-to-peptide proton transfer, while the second one was taken as evidence against the laser-induced ionization as the mechanism for the matrix ion formation. Motivated by a claim that the gas-phase ion formation in DHB-MALDI is initiated by laser-induced ionization of DHB, we performed a similar study on this case. Based on the data that we obtained, we conclude that there is no evidence to support different primary ion formation mechanisms between the two matrices. To put it more explicitly, primary ions in both cases are formed *via* a thermal process(es) in the ground electronic state, not *via* an exotic exited state chemistry such as the one mediated by exciton pooling.

Table 3. The number of DHB-derived positive ions and ionization efficiencies of DHB *vs.* laser wavelength and pulse energy in DHB-MALDI

Wavelength	Power,[a] μJ/pulse	Number of ions from sample[b] DHB, 10^9	Ionization[b] efficiency DHB, 10^{-8}
317 nm	13.8 (×6)	1.5±0.5 (2.0±0.6)	2.9±0.9 (3.8±1.1)
	23.0 (×10)	1.5±0.4 (2.2±0.6)	2.9±0.7 (4.2±1.3)
337 nm	9.90(×6)	1.3±0.2 (2.0±0.3)	2.5±0.5 (3.8±0.4)
	13.8 (×8.5)	1.4±0.4 (2.0±0.5)	2.8±0.6 (4.0±0.9)
	16.5 (×10)	1.2±0.3 (1.9±0.3)	2.4±0.6 (3.7±0.6)
357 nm	9.78(×6)	1.5±0.4 (2.1±0.5)	2.9±0.7 (4.0±0.9)
	13.8 (×8.4)	1.5±0.3 (2.0±0.5)	2.9±0.7 (4.0±0.9)
	16.3 (×10)	1.5±0.3 (2.1±0.3)	3.0±0.4 (4.2±0.5)

[a]Numbers inside parentheses denote the pulse energy in unit of the threshold value. [b]Numbers inside parentheses denote the values estimated by including alkali metal ion adducts.

References

1. Hillenkamp, F.; Peter-Katalinić, J. *MALDI MS. A Practical Guide to Instrumentation, Methods and Applications*; Wiley-VCH:

Weinheim, Germany, 2007.

2. Dreisewerd, K. *Chem. Rev.* **2003**, *103*, 395.
3. Cole, R. B. *Electrospray and MALDI Mass Spectrometry Fundamentals, Instrumentation, Practicalities, and Biological Applications*, 2nd ed.; John Wiley & Sons: Hoboken, New Jersey, 2010.
4. Knochenmuss, R. *Analyst.* **2006**, *131*, 966.
5. McCombie, G.; Knochenmuss, R. *J. Am. Soc. Mass Spectrom.* **2006**, *17*, 737.
6. Chen, X.; Carroll, J. A.; Beavis, R. C. *J. Am. Soc. Mass Spectrom.* **1998**, *9*, 885.
7. Niu, S.; Zhang, W.; Chait, B. T. *J. Am. Soc. Mass Spectrom.* **1998**, *9*, 1.
8. Bae, Y. J.; Park, K. M.; Kim, M. S. *Anal. Chem.* **2012**, *84*, 7107.
9. Bae, Y. J.; Shin, Y. S.; Moon, J. H.; Kim, M. S. *J. Am. Soc. Mass Spectrom.* **2012**, *23*, 1326.
10. Bae, Y. J.; Moon, J. H.; Kim, M. S. *J. Am. Soc. Mass Spectrom.* **2011**, *22*, 1070.
11. Demeure, K.; Gabelica, V.; De Pauw, E. A. *J. Am. Soc. Mass Spectrom.* **2010**, *21*, 1906.
12. Demeure, K.; Quinton, L.; Gabelica, V.; De Pauw, E. *Anal. Chem.* **2007**, *79*, 8678.
13. Knochenmuss, R.; Zhigilei, L. V. *J. Mass Spectrom.* **2010**, *45*, 333.
14. Strupat, K.; Karas, M.; Hillenkamp, F. *Int. J. Mass Spectrom. Ion Processes* **1991**, *111*, 89.
15. Ha, M.; In, Y.; Maeng, H.; Zee, O. P.; Lee, J.; Kim, Y. *Mass Spectrom. Lett.* **2011**, *2*, 61.
16. Bae, Y. J.; Yoon, S. H.; Moon, J. H.; Kim, M. S. *Bull. Korean Chem. Soc.* **2010**, *31*, 92.
17. Moon, J. H.; Shin, Y. S.; Bae, Y. J.; Kim, M. S. *J. Am. Soc. Mass Spectrom.* **2012**, *23*, 162.
18. Yoon, S. H.; Moon, J. H.; Kim, M. S. *J. Am. Soc. Mass Spectrom.* **2010**, *21*, 1876.
19. Moon, J. H.; Yoon, S. H.; Kim, M. S. *J. Phys. Chem. B* **2009**, *113*, 2071.
20. Mowry, C. D.; Johnston, M. V. *Rapid Commun. Mass Spectrom.* **1993**, *7*, 569.
21. Quist, A. P.; Huth-Fehre, T.; Sundqvist, B. U. R. *Rapid Commun. Mass Spectrom.* **1994**, *8*, 149.
22. Allwood, D. A.; Dreyfus, R. W.; Perera, I. K.; Dyer, P. E. *Rapid Commun. Mass Spectrom.* **1996**, *10*, 1575.
23. Westmacott, G.; Ens, W.; Hillenkamp, F.; Dreisewerd, K.; Schürenberg, M. *Int. J. Mass Spectrom.* **2002**, *221*, 67.
24. Zhigilei, L. V.; Leveugle, E. *Chem. Rev.* **2003**, *103*, 321.